Dentomaxillofacial Radiology (2021) 50, 20200503

birpublications.org/dmfr

RESEARCH ARTICLE

Influence of CBCT-based volumetric distortion and beam hardening artefacts on the assessment of root canal filling quality in isthmus-containing molars

[1]Clarissa Teles Rodrigues, [2,3,4]Reinhilde Jacobs, [2,3]Karla Faria Vasconcelos, [5,6]Paul Lambrechts, [7]Izabel Regina Fisher Rubira-Bullen, [8]Hugo Gaêta-Araujo, [9]Christiano Oliveira-Santos and [1]Marco Antonio Hungaro Duarte

[1]Department of Restorative Dentistry, Endodontics and Dental Materials, Bauru School of Dentistry, University of São Paulo, São Paulo, Brazil; [2]Department of Imaging and Pathology, Faculty of Medicine, OMFS IMPATH Research Group, KU Leuven, Leuven, Belgium; [3]Department of Oral and Maxillofacial Surgery, University Hospitals Leuven, Leuven, Belgium; [4]Department of Dental Medicine, Karolinska Institutet, Stockholm, Sweden; [5]Department of Oral Health Sciences, Endodontology, KU Leuven and Dentistry, University Hospitals Leuven, Leuven, Belgium; [6]Biomaterials-BIOMAT, Leuven, Belgium; [7]Department of Surgery, Stomatology, Pathology and Radiology, Bauru School of Dentistry, University of São Paulo, São Paulo, Brazil; [8]Division of Oral Radiology, Department of Oral Diagnosis, Piracicaba Dental School, University of Campinas, São Paulo, Brazil; [9]Department of Stomatology, Public Oral Health, and Forensic Dentistry, School of Dentistry of Ribeirão Preto, University of São Paulo, Ribeirão Preto, Brazil

Objectives: To evaluate the influence of artefacts in cone beam CT (CBCT) images of filled root canals in isthmus-containing molars.
Methods: 10 teeth presenting canals with an isthmus were instrumented and filled with a thermoplasticised obturation technique. The teeth were scanned using a micro-CT device and two CBCT devices: 3D Accuitomo 170 (ACC) and NewTom VGi evo (NT), with different acquisition protocols: larger and smaller voxel size. Three examiners assessed the CBCT images for: (1) detection of filling voids; (2) assessment of under- or overestimation of the filling material and (3) resemblance of CBCT images to the reference standard. Analyses of Task 1 yielded accuracy, sensitivity and specificity for detection of filling voids. For tasks 2 and 3, statistical analysis was performed using Wilcoxon test. The level of significance was set at $p < .05$.
Results: For Task 1, ACC showed higher sensitivity, whereas NT presented higher specificity. No significant difference was found between the protocols in ACC, however, for NT, differences between protocols were significant for all diagnostic values. In Task 2, visualisation of the filling was overestimated for NT, while for ACC, underestimation was observed. For Task 3, images with smaller voxel size were more similar to the reference image, for both CBCT devices.
Conclusions: Different artefacts compromise the detection of filling voids on CBCT images of canals in mandibular molars with isthmus. ACC and NT present rather similar diagnostic accuracy, even though artefact expression remains device-specific.
Dentomaxillofacial Radiology (2021) **50**, 20200503. doi: 10.1259/dmfr.20200503

Cite this article as: Rodrigues CT, Jacobs R, Vasconcelos KF, Lambrechts P, Rubira-Bullen IRF, Gaêta-Araujo H, et al. Influence of CBCT-based volumetric distortion and beam hardening artefacts on the assessment of root canal filling quality in isthmus-containing molars. *Dentomaxillofac Radiol* 2021; **50**: 20200503.

Keywords: Artefacts; Cone-beam computed tomography; Microcomputed tomography; Root canal obturation.

Correspondence to: Clarissa Teles Rodrigues, E-mail: clarit@uol.com.br

Received 16 October 2020; revised 29 November 2020; accepted 08 December 2020

Introduction

When root canal fillings fail to provide an adequate sealing, leakage of fluids can provide substrate for bacterial growth inside the root canal system, jeopardising the long-term success of the endodontic treatment.[1]

However, complete filling of the root canal is a challenge during endodontic treatment, especially when anatomical complexities, such as isthmuses, are present.[2] The presence of an isthmus is a common finding in mandibular molars,[3,4] compromising proper cleaning and disinfection of the root canal system[5,6] because of the difficulty in reaching these areas.[7] Furthermore, debris packed in this area after root canal instrumentation may prevent adaptation of filling materials and influence root canal obturation quality.[2,8–10]

Conventional radiographs are commonly used for evaluating the quality of the endodontic treatment, nevertheless voids in the root filling may be masked considering two-dimensional anatomical overlap.[11,12]

The drawbacks related to superimposition may be overcome by the use of cone beam CT (CBCT). Endodontic applications have increased over the last decade, including visualisation of anatomically complex root canal systems, root resorption, obliterated canals, root fractures, complications of previous treatments establishing retreatment options, image-guided endodontics and detection of periapical pathologies.[13,14] Obviously, the above-mentioned justifications only apply when diagnostic information and/or potential treatment benefits overweigh the risk of ionising radiation exposure.[14,15]

One major obstacle in endodontic post-treatment diagnosis using CBCT, is the presence of artefacts deriving from gutta-percha and sealers and/or other hyperdense materials. Artefacts are distortions or errors in the reconstructed data shown as structures that are not present in the real object.[16,17] These artefacts can appear as different patterns, such as streaks, hypodense halo, and shadows oriented along the projection lines.[17] Such artefacts are mainly related to the beam hardening phenomenon, reducing image quality and consequently diagnostic capability.[17–21] Intracanal filling materials may also cause volumetric distortion or blooming, leading to overestimation of the obturations as perceived on CBCT.[17,20,21] Combinations of artefacts may compromise diagnostic accuracy of voids and perforations.[11,22–24]

Different procedures have been suggested to reduce artefacts and improve image quality, related to the selection of optimal scanning parameters during image acquisition or the use of specific reconstruction algorithms. It has been reported that the use of higher kVp,[25] higher mA,[26] metal artefact reduction algorithms,[25] and restricted field of view[27] with the target object in its center[19] may result in less artefact formation in some CBCT devices.

Spatial resolution is another factor that determines image quality because it is related to the capacity of distinguishing small structures on a CBCT image.[28,29] It also plays an important role in the occurrence of blooming artefacts.[30] It is determined by many factors, including the reconstructed voxel size.[29] Images acquired with smaller voxel sizes (high-resolution) provide more detail and are preferred to visualise complex anatomy such as the mesiobuccal canal system[31] and root fracture lines.[18,19] Yet, one should be aware that such high-resolution protocol involves increased radiation dose.[30]

One structure that is important for adequate endodontic treatment is the isthmus area of multirooted teeth. The isthmus area of mandibular molars presents significantly more voids compared with the main root canals after root canal obturation.[9] However, as far as we know, there is no study regarding the visualisation of voids in the isthmus area using CBCT devices with different resolutions. Thus, the aim of this study was to assess the influence of CBCT protocols and related artefacts on the visualisation of root canal fillings in isthmus-containing molars.

Methods and materials

Tooth selection

The study was approved by local research ethics committee (protocol 86782418.5.0000.5417). Human mandibular molars obtained from institutional pool of extracted teeth were scanned in a micro-computed tomography (micro-CT) unit (SkyScan 1174; SkyScan, Bruker, Kontich, Belgium) with a 22.9 µm voxel size, 50 kVp, 800 µA and 1.0 step rotation, in order to search for mesial roots with the presence of isthmus. Teeth with incomplete rhizogenesis, internal or external resorption, root fractures, C-shaped or calcified root canals, and endodontic treatment were excluded. For the sample calculation, the G*Power v. 3.1 for Mac (Heinrich Heine Universität Düsseldorf) was used and the Wilcoxon–Mann–Whitney test of the *t* test family was selected. The data of a previous study that evaluated the detection of an isthmus in mandibular molars[32] were used and the effect size in the present study was established (=1.36). The α type error of 0.05, a β power of 0.80, and a ratio N2/N1 of 1 were also stipulated. A total of nine samples per group were indicated as the ideal size required for noting significant differences. 10 samples were used, considering 10% of risk of loss of sample. 10 teeth with mesial roots presenting canals classified as Type I according to Vertucci[33] connected by a single and continuous isthmus, *i.e.* Type V according to Hsu & Kim[34], were selected.

Teeth preparation

Coronal access was performed by using diamond burs. The working length was established by introducing a 10-Kfile until its tip was visible at the apical foramen,

and the working length was set at 1.0 mm short of this measure. Tooth apices were sealed with hot glue and embedded in silicone impression material polyvinyl siloxane (Zetaplus, Zhermack, Italy), to simulate the effect of apical gas entrapment in a closed canal system during root canal preparation.[35]

Root canals were instrumented with Reciproc R25 files (VDW GmbH, Munich, Germany) in a reciprocating motion by using an electric motor (VDW Silver; VDW GmbH, Munich, Germany) using the configuration "Reciproc ALL". The instrument was moved in apical direction using an in-and-out pecking motion of about 3 mm in amplitude with slight apical pressure. After three pecking motions, the instrument was removed from the canal and cleaned. A single operator with expertise in performing root canal treatment using reciprocating techniques performed all the preparations. Root canals were irrigated with 5 ml 3% NaOCl, 5 ml 17% EDTA and 3% NaOCl, respectively by using a 30 G Navitip needle (Ultradent, South Jordan, UT). Then, each canal was dried with absorbent paper points (Reciproc R25 paper points, VDW GmbH, Munich, Germany).

Root canal filling

Root canals were filled using Calamus Dual (Dentsply, Maillefer, Ballaigues, Suíça), according to Marciano et al[2], with modifications.

A master gutta-percha cone Reciproc R25 (VDW, Munich, Germany) was selected and inserted into the root canal with AH Plus sealer (Dentsply Maillefer) up to the working length. AH Plus sealer was selected for all samples due to its properties, as high radiopacity, and flowability, which could favour the filling of isthmus area.[36–38] The root canals were filled using a size B endodontic finger spreader (Dentsply Maillefer) inserted 2 mm short of the working length and accessory gutta-percha points size 20 and 0.02 taper (Dentsply Maillefer) were used. A Calamus plugger set at 200°C was used to cut the gutta-percha cone at the orifice level. Schilder hand pluggers (Odus De Deus, Belo Horizonte, Minas Gerais, Brazil) were used to adapt the gutta-percha at the orifice level. The downpack procedure was performed introducing a 50/0.05 Calamus plugger in a continuous wave of condensation within 4 mm of the working length. The plugger was held in position for 10 s before the Calamus was activated for 1 s and withdrawn from the tooth. Gutta-percha at the apical level was condensed using Schilder hand pluggers. The backfill of the coronal portion was achieved using the extruded handpiece and 20 G needle tips containing gutta-percha at a temperature of 200°C and condensed with the appropriate hand pluggers.

Buccolingual and mesiodistal radiographs were taken to confirm that all specimens had well-compacted fillings extending to 1 mm short of the apex, using Minray intraoral X-ray tube (Soredex, Tuusala, Finland) with phosphor plates - size 2 (Digora, Optime, Soredex). Coronal access was sealed with temporary filling material (Coltosol; Coltene-Whaledent, Cuyahoga Falls, OH) and teeth were stored at 37°C and 100% humidity for 7 days to allow complete setting of the sealer.

Micro-CT image acquisition

Subsequently, the teeth were scanned by using a micro-CT device (SkyScan 1172, Bruker, Kontich, Belgium) for the visualisation of the root canal obturation and the filling of the isthmus area. The scanning parameters were set at 100 kVp, 100 µA, 360° rotation, 0.5 mm Al filter, 0.7 step rotation and an isotropic voxel of 12.8 µm. Images were reconstructed using NRecon software (v. 1.6.9.8; Bruker micro-CT) with a beam-hardening correction of 60%, smoothing of 3 and ring artefact correction of 8, and saved as bitmap (BMP) format. The micro-CT images were used as the reference standard of the presence of filling material in isthmus-containing mesial roots of mandibular molars.

CBCT image acquisition

The same teeth were individually placed in empty tooth sockets of a dry human mandible. The socket was carefully enlarged with a cylindrical bur to obtain passive fit for all roots. In order to simulate the attenuation of soft tissue during the CBCT scans, the mandible was covered with 1 cm of a mixture called Mix-D.[39] The mandible was subsequently scanned selecting clinical reference settings available on CBCT devices, typically advised for endodontic protocols: NewTom VGi evo (NT) (Cefla S. C., Imola, Italy) and 3D Accuitomo 170 (ACC) (J. Morita, Kyoto, Japan). Two different acquisition protocols were used for each CBCT device: with larger voxel size (0.2 mm for both devices) and smaller voxel size (0.1 mm for NT and 0.08 mm for ACC) (Table 1). Images were exported as digital imaging and communications in medicine (DICOM) files.

CBCT and Micro-CT images evaluation

Image registration was performed using Amira software 6.1.1 (Thermo Fisher Scientific, Berlin, Germany) in order to align the anatomical landmarks on CBCT and micro-CT images for each tooth. After that, the registered images were exported in DICOM format to Image J software (Java, Wayen Rasband, U.S. National Institutes of Health, Bethesda, MD) and matching axial

Table 1 Aquisition parameters selected for each CBCT device

	Accuitomo		*NewTom VGi Evo*	
	Hi-Fidelity	*Hi-Resolution*	*Hi-Resolution*	*Standard*
mA	5	5	3	3
kVp	90	90	110	110
FOV	4 × 4	4 × 4	5 × 5	5 × 5
Voxel size	0.08	0.2	0.1	0.2

CBCT, cone beam CT; FOV, Field of view (cm); VS, Voxel size (mm); VS, Voxel size; kVp, Tube voltage; mA, Tube current.

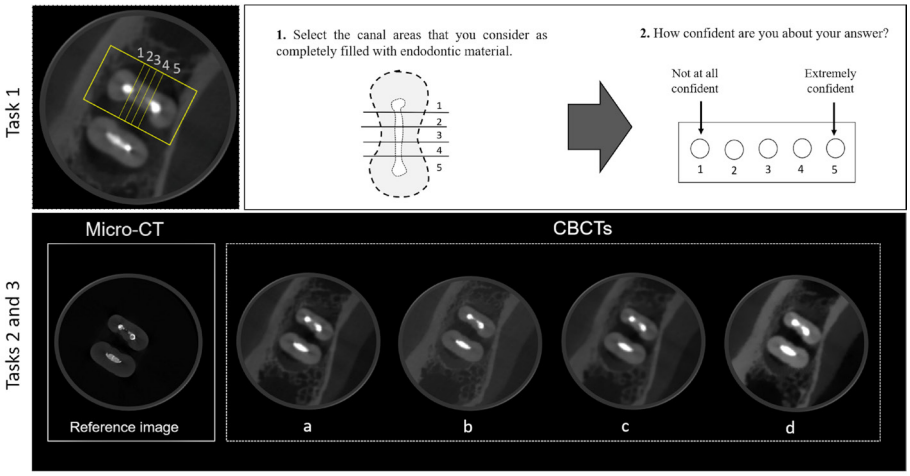

Figure 1 Representative image of an axial slice of CBCT (on top) showing the root canal in the mesial root divided into five regions for the assessment of presence of filling voids during Task 1. Scheme of a mesial root used for examiner´s calibration (1). Visual analogue scale used to indicate the examiner´s level of confidence (2). Representative set of slices of a sample (below), showing the same tooth on micro-CT and different CBCT devices and protocols, for blind evaluation in tasks 2 and 3. CBCT, cone beam CT.

slices from all protocols were selected for evaluation. Slices were exported using the smallest slice thickness, while window level adaptation was not allowed.

Evaluation of the images consisted of three different tasks performed by three experienced Oral and Maxillofacial radiologists, after proper calibration regarding the protocol for each task.

Task 1

Task 1: detection of filling voids and confidence level: Two axial slices from the coronal, middle and apical thirds were selected from each tooth, totaling 60 slices. On each axial slice, the canal of the mesial root was divided into five regions of interest. Examiners classified each region of interest of the root canal on the axial slices according to the absence or presence of filling voids (*i.e.* area completed filled or partially/not filled, respectively). Moreover, for each axial slice, the examiners pointed out how confident they were concerning their answers, in a visual analogue scale (VAS), based on a previous study[39] (Figure 1).

The micro-CT axial slices matching those from CBCT served as the reference standard, and were independently evaluated by two experts, one specialist in Oral and Maxillofacial Radiology and one specialist in Endodontics, using the same aforementioned criteria. In case of disagreement, images were re-examined, and consensus was reached between both experts.

Task 2

Task 2: assessment of underestimation/overestimation of the filling material: This assessment consisted of judging an image panel with all four CBCT images as compared to the reference micro-CT image (Figure 1). For that, 20 image panels (out of 60) were prepared with four registered images slices from the 4 CBCT protocols presented in the same panel with the micro-CT reference image. In this case, three examiners evaluated each image protocol in relation to the reference micro-CT image (representing the clinical reality). For each CBCT image the observer scored if the filling material inside the isthmus was similar to the reference images (0), underestimated (1), or overestimated (2).

Task 3

Comparisons between the CBCT images regarding their resemblance to the reference standard: The examiners evaluated the same 20 images used for Task 2, and ranked the images that better depicted the filling of the isthmus area, using the micro-CT as reference, i.e. which image most closely resembled the actual clinical anatomical condition (Figure 1).

All observation sessions were performed in a dimly lit room with a medical monitor (Barco MDRC-2221, Kortrijk, Belgium). Neither contrast and brightness adaptations nor enhancement filter application were allowed. 20% of the images were re-evaluated after a 15-day interval in order to calculate intraexaminer agreements. Examiners were blinded regarding the acquisition protocols, CBCT machine, and presence of filling voids.

Statistical analysis

Considering micro-CT as reference standard, for the first task the diagnostic values (*i.e.* accuracy, sensitivity, and specificity) of each CBCT device and protocols were calculated for each third of the root canal. Regions of interest 1 and 5, which are related to the main canal,

Table 2 Prevalence of filling voids detected on micro-CT images, according to region of interest and root canal third

	Region of interest				
Root canal third	*1*	*2*	*3*	*4*	*5*
Coronal	0	11	14	2	1
Middle	3	9	10	6	1
Apical	0	11	8	10	1
Total	3 (5%)	31 (51.7%)	32 (53.3%)	18 (30%)	3 (5%)

presented filling voids in only 3 out of 60 slices and were excluded because the calculation of diagnostic values for those regions was impaired. Therefore, the diagnostic values correspond to those obtained from regions of interest 2, 3, and 4, which are representative of the isthmus in those canals. Overall diagnostic values were compared between protocols within each CBCT device (*t*-test) and according to root thirds (two-way ANOVA).

The results of the VAS were calculated for each observer and expressed in relative frequencies. These results representing self-reported confidence levels were calculated for "correct diagnosis" and "incorrect diagnosis" separately, *i.e*. how confident were the observer for the cases where the CBCT observations were in agreement or disagreement with those from micro-CT.

Distribution of the ranking from the tasks 2 and 3 were compared between protocols, within each CBCT device, by Wilcoxon signed-rank test.

κ test was used to assess inter- and intraexaminer agreement.

The level of significance was set at $p < .05$. Analysis were performed with GraphPad Prism 5 (GraphPad Software Inc, La Jolla, CA) and SPPS Statistics software v. 22.0 (IBM Corp., Armonk, NY).

Results

The prevalence of filling voids observed on micro-CT images are shown in Table 2. Filling voids were present in only 5% of regions of interest 1 and 5. Combined, regions of interest 2, 3, and 4, representative for the isthmus, presented voids in 45% of the cases. For CBCT analysis, inter- and intraobserver agreement were on average 0.87 and 0.92 (almost perfect agreement).

For Task 1, sensitivity, specificity and accuracy for each CBCT protocol and according to root thirds are presented in Table 3. Overall, ACC presented sensitivity much higher than specificity, whilst NT showed very low sensitivity and very high specificity. For ACC, no significant differences in diagnostic values were found between the protocols tested ($p > .05$), and, although accuracy was similar among the root thirds, sensitivity was very high, while specificity being low for the cervical third but considerably higher for the apical part. For the NT device, differences between protocols were significant for all diagnostic values. Sensitivity was significantly lower in the apical third, whilst specificity was very high in all thirds. For answers in agreement with the micro-CT reference, the level of confidence ranged from 77 to 92%, for answers not in agreement with the micro-CT reference it ranged from 74 to 93% (Figure 2).

Regarding the analysis of Task 2, no difference was found between protocols within each CBCT device ($p > .05$). In general, visualisation of the filling was overestimated for NT, while ACC showed a slight underestimation of the filling (Figure 3). For Task 3, images with smaller voxel size were more similar to the reference micro-CT image, for both ACC ($p = .009$) and NT ($p < .001$) (Figure 3).

Table 3 Diagnostic values calculated for the detection of filling voids in each root canal third, among the different CBCT protocols tested

		CBCT protocols – mean (SD)			
Diagnostic values	*Root canal third*	*Accuitomo 0.08 mm*	*Accuitomo 0.2 mm*	*NewTom 0.1 mm*	*NewTom 0.2 mm*
Sensitivity	Coronal	0.889 (0.06)^{A}	0.889 (0.06)^{A}	0.370 (0.07)^{A}	0.358 (0.06)^{A}
	Middle	0.693 (0.05)^{B}	0.653 (0.06)^{B}	0.213 (0.02)^{Ba}	0.080 (0.00)^{Ba}
	Apical	0.494 (0.05)^{C}	0.448 (0.03)^{C}	0.126 (0.07)^{C}	0.000 (0.00)^{B}
	Overall	0.687 (0.05)	0.658 (0.05)	0.226 (0.04)^{a}	0.144 (0.02)^{a}
Specificity	Coronal	0.273 (0.08)^{A}	0.273 (0.03)^{A}	1.0 (0.00)^{A}	0.970 (0.00)^{A}
	Middle	0.514 (0.03)^{B}	0.524 (0.04)^{B}	1.0 (0.00)^{A}	0.933 (0.02)^{A}
	Apical	0.699 (0.04)^{C}	0.731 (0.02)^{C}	1.0 (0.00)^{A}	0.988 (0.02)^{A}
	Overall	0.492 (0.02)	0.505 (0.03)	1.0 (0.0)^{a}	0.963 (0.01)^{a}
	Coronal	0.550 (0.06)^{A}	0.550 (0.03)^{A}	0.717 (0.03)^{A}	0.694 (0.03)^{A}
Accuracy	Middle	0.589 (0.03)^{A}	0.578 (0.05)^{A}	0.672 (0.01)^{Ba}	0.578 (0.01)^{Ba}
	Apical	0.600 (0.02)^{A}	0.594 (0.02)^{A}	0.567 (0.02)^{B}	0.511 (0.01)^{C}
	Overall	0.580 (0.03)	0.574 (0.03)	0.652 (0.02)^{a}	0.594 (0.01)^{a}

CBCT, cone beam CT.
Different superscript capital letters indicate statistically significant difference between root thirds, within each protocol.
^{a}indicates statistically significant difference between protocols within the same CBCT machine.

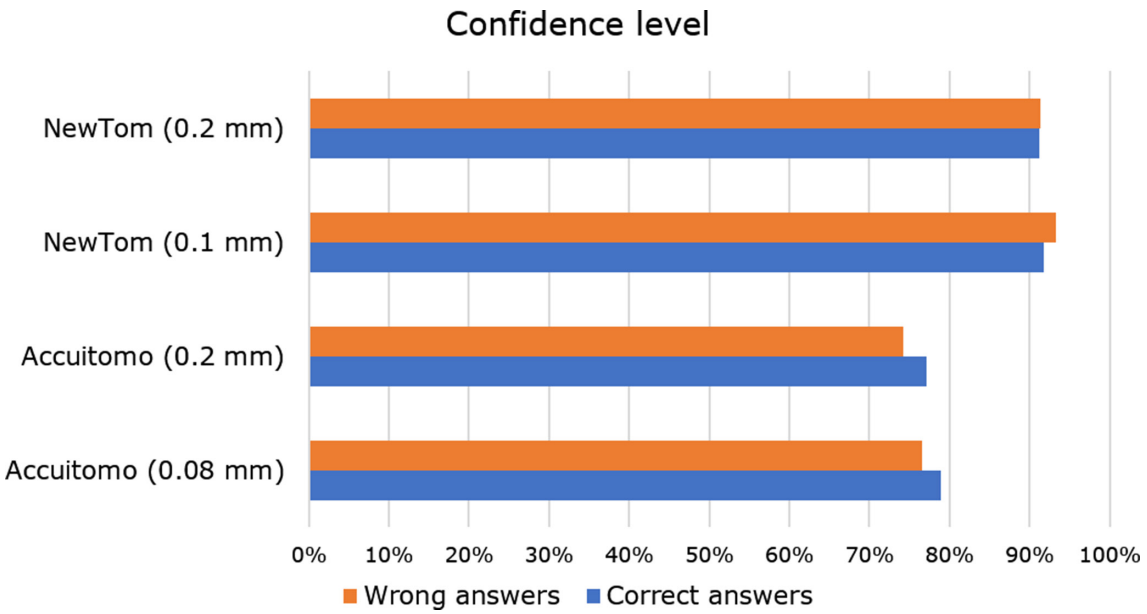

Figure 2 Confidence levels for the observers and CBCT protocol, and according to correct or incorrect diagnosis (*i.e.* when the diagnosis provided by the observer was in agreement or disagreement, respectively, with micro-CT findings). Confidence levels are represented by the relative frequency of cases where the observers reported that they were confident about their diagnosis. CBCT, cone beam CT.

Discussion

CBCT imaging is recommended for the assessment of anatomically complex root canal systems and previous treatment complications in cases when conventional radiography is not sufficient.[12,14] The present study was designed to assess root canal filling quality in isthmus-containing molars by using endodontic acquisition protocols. However, it is important to stress that the study did not intend to compare the performance of CBCT devices, but rather the potential and limitations of different CBCT protocols to visualise the actual clinical situation considering micro-CT as standard reference. The CBCT devices selected were those with high resolution and low metal artefact problems, typically used for post-endodontic assessments,[21] even though findings remain CBCT- and task specific.[14,39] Yet and even then, void assessment remained moderate, potentially related to artefact expression and near-threshold detections specifically related to the present task.

Detection of filling voids is of utmost importance in clinical practice, even the small ones, which are more likely to occur regardless of the filling technique used.[2,11] A micro-CT and nano-CT study showed that higher resolutions produce more detailed information about presence of voids in tomographic images.[40] In a clinical situation, in which an unsuccessful endodontic treatment is suspected, it is necessary to assess the quality of root canal obturation for re-treatment planning or investigate the causes of failure, to avoid planning errors, such as unnecessary tooth extraction.

Regarding the diagnostic values, for the NT device, it was found that an increase in resolution, *i.e.* from 0.2 to 0.1 mm voxel size, positively affected the overall accuracy for the detection of filling voids. While for ACC no significant differences were found between the protocols 0.2 and 0.08 mm ($p > .05$). Neves et al[41] also found that different imaging modes in ACC did not influence diagnosis of vertical root fractures in teeth filled with gutta-percha. The present observations may imply that initial ACC images are already scanned at high resolution, not demanding a further increase in the imaging parameters and likewise radiation dose.

Artefacts related to high-density intracanal materials, including gutta-percha and sealers, may have serious clinical implications because they can lead to false interpretations and misdiagnosis.[16,22,24,41–44] In this study, beam hardening artefact may have led to more frequent false-positive detection of filling voids on ACC images, leading to higher sensitivity and lower specificity, particularly in the coronal third of the roots. The filling material is thicker in the coronal third[11] which may lead to more pronounced beam hardening in that root level. The beam hardening artefact may also have led ACC images to possibly underestimate the filling in comparison with the real condition, which was confirmed in Task 2 of this study. A previous report showed a likewise impairment in visualisation of these areas of interest in CBCT images related to dark bands associated with intracanal endodontic material.[17]

On the other hand, volumetric distortion or blooming artefact represents an overestimation in the volume of the filling material. The very low sensitivity and very high specificity of NT images for this diagnostic task may be explained by a predominance of blooming artefacts. Higher values of specificity indicate capability of correctly identifying completely filled areas. Nevertheless, these lower values of sensitivity indicate

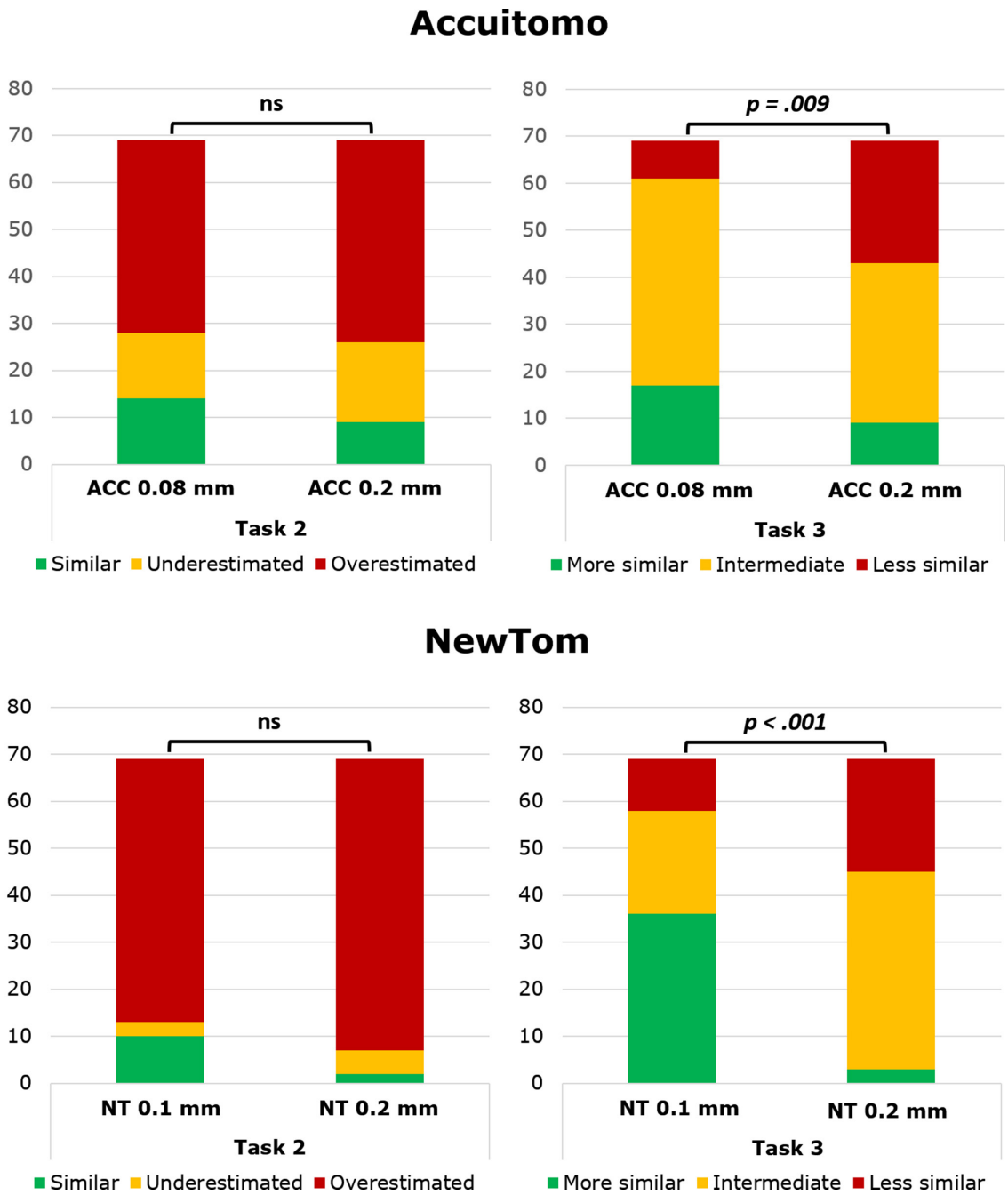

Figure 3 Bar graphs showing the distribution of the ranking for tasks 2 and 3 for both CBCT devices, in comparison to a micro-CT reference image. *p* values according to Wilcoxon signed-rank test. CBCT, cone beam CT; Ns, Non-significant.

that voids are generally not easily identified. Increased volumetric distortion of the root filling material when comparing NT with micro-CT has also been reported in the literature.[20,21]

Due to the phenomenon of blooming artefact, the expansion of the filling material easily occupies the space of this small void, leading to a false impression that the root canal is completed filled or to a false diagnosis of perforations (Figure 4). The apical third yielded the lowest sensitivity, which may be related to the limited thickness of the dentin in this root level. For this device, the blooming artefact affected more the apical third than the coronal third, with lower values of sensitivity found in this region, which was more pronounced with a larger voxel protocol. The apical third presents a small area compared with the coronal third, with smaller voids, observed in the micro-CT images. The identification of more overestimated conditions in Task 2 of this study confirmed that the blooming artefact was more evident in images acquired with NT device.

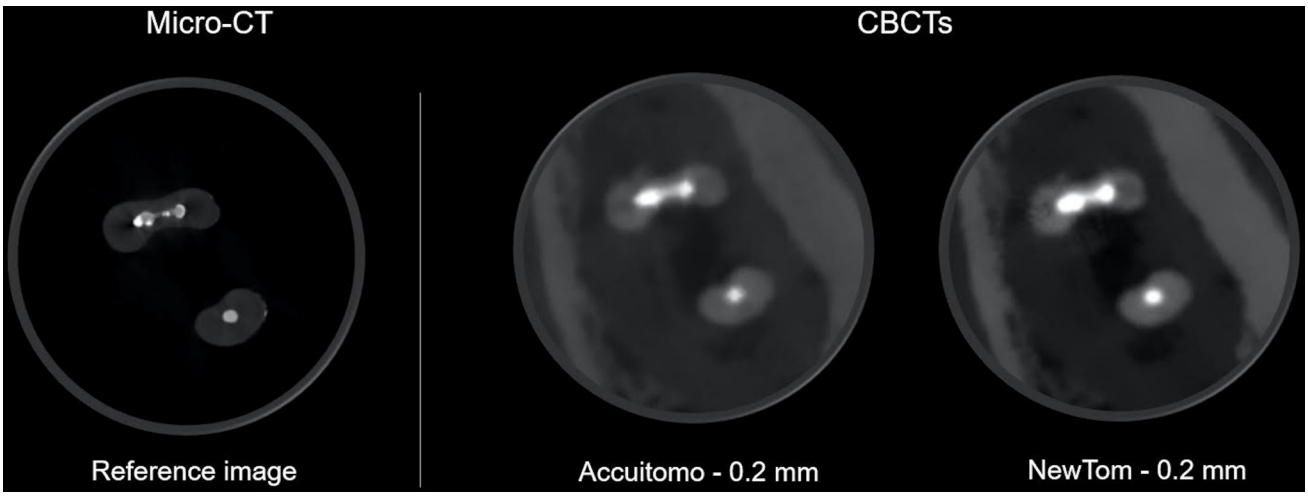

Figure 4 Representative CBCT images of a sample acquired with larger voxel protocols demonstrating that the blooming artefact may simulate a root canal perforation, which is not evidenced in the micro-CT image. CBCT, cone beam CT.

The results from the VAS related to the examiner's confidence level, showed that the observers were more confident about their diagnosis with NT images, both when they had correct or incorrect diagnoses of filling voids. The decisiveness of the professional influences the treatment plan of the patient. If one judges correctly, but is not sure about the answer, he/she may probably order unnecessary additional exams. On the contrary, if one judges erroneously, but is overconfident about the decision, he/she may indicate unnecessary or erroneous procedures.[45] This can lead to clinicians making wrong decisions during treatment planning, either re-treatment, extraction or not making any intervention in the treated root canal. It is important to notice that other factors may be related to the decision ability of the examiners, such as the examiner's experience and their knowledge about the limitation of CBCT images. Therefore, the results of the VAS were not compared between the three examiners in this study, since this comparison is not clinically relevant and could lead to misinterpretation.

To score the quality of obturation in this study, the root canal was divided into five areas. It was observed on micro-CT that the isthmus area (*i.e.* regions 2, 3 and 4) presented more voids, due to the difficulty in filling this narrow area, which was already demonstrated by previous studies.[2,9] Due to the very low prevalence of voids in regions 1 and 5 (main canal) observed on micro-CT, the scores for these regions were excluded for all analysis.

In our study, smaller voxel sizes protocols, in both CBCT devices, yielded images more similar to the micro-CT in Task 3. The better performance of high-resolution protocols may be attributed to a phenomenon present in CBCT images called partial volume effect (PVE). This condition occurs when two materials with different densities are present in the same voxel, which results in errors during image formation.[46] The PVE may lead to incorrect estimation of the volume occupied by the two materials, especially at the edge of these materials.[46,47] The presence of PVE is reduced when the voxel size is smaller,[48] explaining the significant difference in acquisition protocols of Task 3, *i. e,* images with smaller voxel size were more similar to the reference image.

Another effect that could had influenced CBCT image quality is the noise. In the present study, this could also have hampered perception of filling voids. Exposure settings such as tube current (mA) and voxel size are related to image noise, *i.e.* the lower the mA and the smaller the voxel size, the greater the noise.[49,50] In the current study, pre-set exposures were used with different voxel sizes in the same device, but no variation of mA was observed (Table 1). Therefore, as the mA was constant in the same device, it is expected that images with smaller voxel sizes yielded more noise. It is worth noting that radiation dose is also influenced by mA and voxel size. Further studies are needed to assess the true impact of the aforementioned variables.

Some limitations are inherent to this *in vitro* experimental study design, such as the use of a dry skull phantom and consequently, the absence of patient-related artefacts (i.e motion artefact). Nevertheless, use of Mix-D cover material allowed reproduction of a very similar tomographic density of human soft tissue.[39] The fact that CBCT image evaluations were performed in pre-defined registered regions should also be highlighted. Although this methodology does not reproduce the volumetric assessment in the clinical practice, it avoids examiner variability, allowing a more controlled and standardised method.[39]

Conclusion

Different artefacts compromise the detection of filling voids on CBCT images of canals in mandibular molars with isthmus. Although both devices reached the same

diagnostic accuracy, artefact expression is device-specific. Additionally, smaller voxel sizes protocols yielded images more similar to the real condition in both CBCT devices.

Acknowledgements

The authors deny any conflict of interests. This study was supported by Conselho Nacional de Desenvolvimento Científico e Tecnológico (CNPq) (150046/2018-9).

REFERENCES

1. Siqueira JF. Aetiology of root canal treatment failure: why well-treated teeth can fail. *Int Endod J* 2001; **34**: 1–10. doi: https://doi.org/10.1046/j.1365-2591.2001.00396.x
2. Marciano MA, Ordinola-Zapata R, Cunha TVRN, Duarte MAH, Cavenago BC, Garcia RB, et al. Analysis of four gutta-percha techniques used to fill mesial root canals of mandibular molars. *Int Endod J* 2011; **44**: 321–9. doi: https://doi.org/10.1111/j.1365-2591.2010.01832.x
3. Villas-Bôas MH, Bernardineli N, Cavenago BC, Marciano M, Del Carpio-Perochena A, de Moraes IG, et al. Micro-computed tomography study of the internal anatomy of mesial root canals of mandibular molars. *J Endod* 2011; **37**: 1682–6. doi: https://doi.org/10.1016/j.joen.2011.08.001
4. Harris SP, Bowles WR, Fok A, McClanahan SB. An anatomic investigation of the mandibular first molar using micro-computed tomography. *J Endod* 2013; **39**: 1374–8. doi: https://doi.org/10.1016/j.joen.2013.06.034
5. Siqueira JF, Alves FRF, Versiani MA, Rôças IN, Almeida BM, Neves MAS, et al. Correlative bacteriologic and micro-computed tomographic analysis of mandibular molar mesial canals prepared by self-adjusting file, reciproc, and twisted file systems. *J Endod* 2013; **39**: 1044–50. doi: https://doi.org/10.1016/j.joen.2013.04.034
6. Urban K, Donnermeyer D, Schäfer E, Bürklein S. Canal cleanliness using different irrigation activation systems: a SEM evaluation. *Clin Oral Investig* 2017; **21**: 2681–7. doi: https://doi.org/10.1007/s00784-017-2070-x
7. Estrela C, Rabelo LEG, de Souza JB, Alencar AHG, Estrela CRA, Sousa Neto MD, et al. Frequency of root canal Isthmi in human permanent teeth determined by cone-beam computed tomography. *J Endod* 2015; **41**: 1535–9. doi: https://doi.org/10.1016/j.joen.2015.05.016
8. Paqué F, Laib A, Gautschi H, Zehnder M. Hard-tissue debris accumulation analysis by high-resolution computed tomography scans. *J Endod* 2009; **35**: 1044–7. doi: https://doi.org/10.1016/j.joen.2009.04.026
9. Endal U, Shen Y, Knut A, Gao Y, Haapasalo M. A high-resolution computed tomographic study of changes in root canal isthmus area by instrumentation and root filling. *J Endod* 2011; **37**: 223–7. doi: https://doi.org/10.1016/j.joen.2010.10.012
10. De-Deus G, Marins J, Neves AdeA, Reis C, Fidel S, Versiani MA, et al. Assessing accumulated hard-tissue debris using micro-computed tomography and free software for image processing and analysis. *J Endod* 2014; **40**: 271–6. doi: https://doi.org/10.1016/j.joen.2013.07.025
11. Huybrechts B, Bud M, Bergmans L, Lambrechts P, Jacobs R. Void detection in root fillings using intraoral analogue, intraoral digital and cone beam CT images. *Int Endod J* 2009; **42**: 675–85. doi: https://doi.org/10.1111/j.1365-2591.2009.01566.x
12. AAE and AAOMR Joint Position Statement. Use of cone beam computed tomography in Endodontics 2015 update. *J Endod* 2015; **41**: 1393–6.
13. Torres A, Shaheen E, Lambrechts P, Politis C, Jacobs R. Microguided Endodontics: a case report of a maxillary lateral incisor with pulp canal obliteration and apical periodontitis. *Int Endod J* 2019; **52**: 540–9. doi: https://doi.org/10.1111/iej.13031
14. Patel S, Brown J, Semper M, Abella F, Mannocci F. European Society of Endodontology position statement: use of cone beam computed tomography in endodontics: European society of endodontology (ESE) developed by. *Int Endod J* 2019; **52**: 1675–8. doi: https://doi.org/10.1111/iej.13187
15. Connert T, Zehnder MS, Amato M, Weiger R, Kühl S, Krastl G. Microguided Endodontics: a method to achieve minimally invasive access cavity preparation and root canal location in mandibular incisors using a novel computer-guided technique. *Int Endod J* 2018; **51**: 247–55. doi: https://doi.org/10.1111/iej.12809
16. Schulze R, Heil U, Gross D, Bruellmann DD, Dranischnikow E, Schwanecke U, et al. Artefacts in CBCT: a review. *Dentomaxillofac Radiol* 2011; **40**: 265–73. doi: https://doi.org/10.1259/dmfr/30642039
17. Vasconcelos KF, Nicolielo LFP, Nascimento MC, Haiter-Neto F, Bóscolo FN, Van Dessel J, et al. Artefact expression associated with several cone-beam computed tomographic machines when imaging root filled teeth. *Int Endod J* 2015; **48**: 994–1000. doi: https://doi.org/10.1111/iej.12395
18. Brito-Júnior M, Santos LAN, Faria-e-Silva AL, Pereira RD, Sousa-Neto MD. Ex vivo evaluation of artifacts mimicking fracture lines on cone-beam computed tomography produced by different root canal sealers. *Int Endod J* 2014; **47**: 26–31. doi: https://doi.org/10.1111/iej.12121
19. Iikubo M, Nishioka T, Okura S, Kobayashi K, Sano T, Katsumata A, et al. Influence of voxel size and scan field of view on fracture-like artifacts from gutta-percha obturated endodontically treated teeth on cone-beam computed tomography images. *Oral Surg Oral Med Oral Pathol Oral Radiol* 2016; **122**: 631–7. doi: https://doi.org/10.1016/j.oooo.2016.07.014
20. Celikten B, Jacobs R, deFaria Vasconcelos K, Huang Y, Nicolielo LFP, Orhan K. Assessment of volumetric distortion artifact in filled root canals using different cone-beam computed tomographic devices. *J Endod* 2017; **43**: 1517–21. doi: https://doi.org/10.1016/j.joen.2017.03.035
21. Celikten B, Jacobs R, de Faria Vasconcelos K, Huang Y, Shaheen E, Nicolielo LFP, et al. Comparative evaluation of cone beam CT and micro-CT on blooming artifacts in human teeth filled with bioceramic sealers. *Clin Oral Investig* 2019; **23**: 3267–73. doi: https://doi.org/10.1007/s00784-018-2748-8
22. Soğur E, Baksi BG, Gröndahl H-G. Imaging of root canal fillings: a comparison of subjective image quality between limited cone-beam CT, storage phosphor and film radiography. *Int Endod J* 2007; **40**: 179–85. doi: https://doi.org/10.1111/j.1365-2591.2007.01204.x
23. Bueno MR, Estrela C, De Figueiredo JAP, Azevedo BC. Map-reading strategy to diagnose root perforations near metallic intracanal posts by using cone beam computed tomography. *J Endod* 2011; **37**: 85–90. doi: https://doi.org/10.1016/j.joen.2010.08.006
24. Decurcio DA, Bueno MR, de Alencar AHG, Porto OCL, Azevedo BC, Estrela C. Effect of root canal filling materials on dimensions of cone-beam computed tomography images. *J Appl Oral Sci* 2012; **20**: 260–7. doi: https://doi.org/10.1590/S1678-77572012000200023
25. Helvacioglu-Yigit D, Demirturk Kocasarac H, Bechara B, Noujeim M. Evaluation and reduction of artifacts generated by 4 different Root-end filling materials by using multiple cone-beam computed tomography imaging settings. *J Endod* 2016; **42**: 307–14. doi: https://doi.org/10.1016/j.joen.2015.11.002
26. Gaêta-Araujo H, Silva de Souza GQ, Freitas DQ, de Oliveira-Santos C. Optimization of tube current in cone-beam computed tomography for the detection of vertical root fractures

with different Intracanal materials. *J Endod* 2017; **43**: 1668–73. doi: https://doi.org/10.1016/j.joen.2017.04.003
27. Costa ED, Brasil DM, Queiroz PM, Verner FS, Junqueira RB, Freitas DQ. Use of the metal artefact reduction tool in the identification of fractured endodontic instruments in cone-beam computed tomography. *Int Endod J* 2020; **53**: 506–12. doi: https://doi.org/10.1111/iej.13242
28. Brüllmann D, Schulze RKW. Spatial resolution in CBCT machines for dental/maxillofacial applications-what do we know today? *Dentomaxillofac Radiol* 2015; **44**: 20140204. doi: https://doi.org/10.1259/dmfr.20140204
29. Pauwels R, Faruangsaeng T, Charoenkarn T, Ngonphloy N, Panmekiate S. Effect of exposure parameters and voxel size on bone structure analysis in CBCT. *Dentomaxillofac Radiol* 2015; **44**: 20150078. doi: https://doi.org/10.1259/dmfr.20150078
30. Pauwels R, Beinsberger J, Collaert B, Theodorakou C, Rogers J, Walker A, et al. Effective dose range for dental cone beam computed tomography scanners. *Eur J Radiol* 2012; **81**: 267–71. doi: https://doi.org/10.1016/j.ejrad.2010.11.028
31. Vizzotto MB, Silveira PF, Arús NA, Montagner F, Gomes BPFA, da Silveira HED. Cbct for the assessment of second mesiobuccal (MB2) canals in maxillary molar teeth: effect of voxel size and presence of root filling. *Int Endod J* 2013; **46**: 870–6. doi: https://doi.org/10.1111/iej.12075
32. Tolentino EdeS, Amoroso-Silva PA, Alcalde MP, Honório HM, Iwaki LCV, Rubira-Bullen IRF, et al. Accuracy of high-resolution small-volume cone-beam computed tomography in detecting complex anatomy of the apical isthmi: ex vivo analysis. *J Endod* 2018; **44**: 1862–6. doi: https://doi.org/10.1016/j.joen.2018.08.015
33. Vertucci FJ. Root canal anatomy of the human permanent teeth. *Oral Surg Oral Med Oral Pathol* 1984; **58**: 589–99. doi: https://doi.org/10.1016/0030-4220(84)90085-9
34. Hsu YY, Kim S. The resected root surface. The issue of canal isthmuses. *Dent Clin North Am* 1997; **41**: 529–40.
35. Susin L, Liu Y, Yoon JC, Parente JM, Loushine RJ, Ricucci D, et al. Canal and isthmus debridement efficacies of two irrigant agitation techniques in a closed system. *Int Endod J* 2010; **43**: 1077–90. doi: https://doi.org/10.1111/j.1365-2591.2010.01778.x
36. Resende LM, Rached-Junior FJA, Versiani MA, Souza-Gabriel AE, Miranda CES, Silva-Sousa YTC, et al. A comparative study of physicochemical properties of AH Plus, Epiphany, and Epiphany SE root canal sealers. *Int Endod J* 2009; **42**: 785–93. doi: https://doi.org/10.1111/j.1365-2591.2009.01584.x
37. Duarte MAH, Ordinola-Zapata R, Bernardes RA, Bramante CM, Bernardineli N, Garcia RB, et al. Influence of calcium hydroxide association on the physical properties of Ah plus. *J Endod* 2010; **36**: 1048–51. doi: https://doi.org/10.1016/j.joen.2010.02.007
38. Candeiro GTdeM, Correia FC, Duarte MAH, Ribeiro-Siqueira DC, Gavini G. Evaluation of radiopacity, pH, release of calcium ions, and flow of a bioceramic root canal sealer. *J Endod* 2012; **38**: 842–5. doi: https://doi.org/10.1016/j.joen.2012.02.029
39. Oenning AC, Pauwels R, Stratis A, De Faria Vasconcelos K, Tijskens E, De Grauwe A, et al. Halve the dose while maintaining image quality in paediatric cone beam CT. *Sci Rep* 2019; **9**: 5521. doi: https://doi.org/10.1038/s41598-019-41949-w
40. Orhan K, Jacobs R, Celikten B, Huang Y, de Faria Vasconcelos K, Nicolielo LFP, et al. Evaluation of threshold values for root canal filling voids in micro-CT and Nano-CT images. *Scanning* 2018; **2018**: 1–6. doi: https://doi.org/10.1155/2018/9437569
41. Neves FS, Freitas DQ, Campos PSF, Ekestubbe A, Lofthag-Hansen S. Evaluation of cone-beam computed tomography in the diagnosis of vertical root fractures: the influence of imaging modes and root canal materials. *J Endod* 2014; **40**: 1530–6. doi: https://doi.org/10.1016/j.joen.2014.06.012
42. Barrett JF, Keat N. Artifacts in CT: recognition and avoidance. *Radiographics* 2004; **24**: 1679–91. doi: https://doi.org/10.1148/rg.246045065
43. Pauwels R, Stamatakis H, Bosmans H, Bogaerts R, Jacobs R, Horner K, et al. Quantification of metal artifacts on cone beam computed tomography images. *Clin Oral Implants Res* 2013; **24 Suppl A100**: 94–9. doi: https://doi.org/10.1111/j.1600-0501.2011.02382.x
44. Codari M, de Faria Vasconcelos K, Ferreira Pinheiro Nicolielo L, Haiter Neto F, Jacobs R. Quantitative evaluation of metal artifacts using different CBCT devices, high-density materials and field of views. *Clin Oral Implants Res* 2017; **28**: 1509–14. doi: https://doi.org/10.1111/clr.13019
45. Dory V, Degryse J, Roex A, Vanpee D. Usable knowledge, hazardous ignorance - beyond the percentage correct score. *Med Teach* 2010; **32**: 375–80. doi: https://doi.org/10.3109/01421590903197027
46. Marinozzi F, Bini F, Marinozzi A, Zuppante F, De Paolis A, Pecci R, et al. Technique for bone volume measurement from human femur head samples by classification of micro-CT image histograms. *Ann Ist Super Sanita* 2013; **49**: 300–5. doi: https://doi.org/10.4415/ANN_13_03_11
47. Chen H, van Eijnatten M, Wolff J, de Lange J, van der Stelt PF, Lobbezoo F, et al. Reliability and accuracy of three imaging software packages used for 3D analysis of the upper airway on cone beam computed tomography images. *Dentomaxillofac Radiol* 2017; **46**: 20170043. doi: https://doi.org/10.1259/dmfr.20170043
48. Scarfe WC, Farman AG. What is cone-beam CT and how does it work? *Dent Clin North Am* 2008; **52**: 707–30. doi: https://doi.org/10.1016/j.cden.2008.05.005
49. Pauwels R, Seynaeve L, Henriques JCG, de Oliveira-Santos C, Souza PC, Westphalen FH, et al. Optimization of dental CBCT exposures through mAs reduction. *Dentomaxillofac Radiol* 2015; **44**: 20150108. doi: https://doi.org/10.1259/dmfr.20150108
50. Al-Rawi B, Hassan B, Vandenberge B, Jacobs R. Accuracy assessment of three-dimensional surface reconstructions of teeth from cone beam computed tomography scans. *J Oral Rehabil* 2010; **37**: 352–8. doi: https://doi.org/10.1111/j.1365-2842.2010.02065.x